

Article

# A QUBO model for the Traveling Salesman Problem with Time Windows for execution on the D-Wave

Christos Papalitsas\*<sup>1</sup>, Theodore Andronikos\*, Konstantinos Giannakis\*<sup>2</sup>, Georgia Theocharopoulou, and Sofia Fanarioti

Department of Informatics, Ionian University, Tsirigoti Square 7, Corfu, 49100, Greece;  
{kgiann, c14papa, zeta.theo, sofiafanar, andronikos}@ionio.gr

\* Correspondence: c14papa@ionio.gr (Ch.P.); andronikos@ionio.gr (Th.A.); kgiann@ionio.gr (K.G.);

‡ These authors contributed equally to this work.

1 **Abstract:** This work focuses on expressing the TSP with Time Windows (TSPTW for short) as a  
2 quadratic unconstrained binary optimization (QUBO) problem. The time windows impose time  
3 constraints that a feasible solution must satisfy. These take the form of inequality constraints, which  
4 are known to be particularly difficult to articulate within the QUBO framework. This is, we believe,  
5 the first time this major obstacle is overcome and the TSPTW is cast in the QUBO formulation. We  
6 have every reason to anticipate that this development will lead to the actual execution of small scale  
7 TSPTW instances on the D-Wave platform.

8 **Keywords:** TSP; TSPTW; Metaheuristics; Quantum Annealing; Ising Model; QUBO; D-Wave

## 9 1. Introduction

10 Quantum computing promotes the exploit of quantum-mechanical principles for computation  
11 purposes. Richard Feynman in 1982 suggested that computation could be done more efficiently by  
12 taking advantage of the power of quantum “parallelism” [1]. Since then quantum computing has  
13 gained a lot of momentum and today appears to be one of the most prominent candidates to partially  
14 replace classical, silicon-based systems. There exist a number of quantum algorithms that run more  
15 efficiently than the best known classical algorithm; arguably, the most famous ones are Shor’s [2] and  
16 Grover’s [3] algorithms. For an in-depth study of quantum computing and quantum information, the  
17 reader is referred to [4].

18 When solving large scale optimization problems, one of the most effective classical strategies is to  
19 search among the nearest neighbors and search for paths between the initial and final configurations  
20 to improve upon an initial guess  $y_t$ . This search takes place locally among neighboring configurations  
21 similar to  $y_t$ . By finding the best solution within the local neighborhood of  $y_t$ , the next candidate  
22 solution  $y_{t+1}$  appears. Then a new local search starts with  $y_{t+1}$  as the starting point in the neighborhood.  
23 Unfortunately, greedy local improvement, in case of hard problems, may be deceptively leading the  
24 solution into a local minima whose energy may be much higher than the globally minimum value.

25 Adiabatic quantum computation was proposed by Farhi et al. [5,6] in the early 2000s [7] and is  
26 based on an important theorem of quantum mechanics, the adiabatic theorem [8,9]. This theorem  
27 dictates that if a quantum system is driven by a slowly changing (in time) Hamiltonian that evolves  
28 from  $H_{init}$  to  $H_{fin}$ , then if the system starts in the ground state of  $H_{init}$ , the system will end up in the  
29 ground state of  $H_{fin}$ . Farhi et al. also showed that adiabatic quantum computation can be efficiently  
30 simulated by a quantum computer based on the gate model, meaning that the two computational  
31 models have the same expressive power [5,6].

32 Quantum annealing is based on the quantum adiabatic computation paradigm. Quantum  
33 annealing was initially proposed by Kadowaki and Nishimori [10,11] and has since then been used  
34 for tackling combinatorial optimization problems. The way that a quantum annealer tries to solve  
35 problems, is very similar to the way optimization problem are solved using (classical) simulated  
36 annealing [12]. An energy landscape is constructed, via a multivariate function, such that the ground  
37 state's coordinates (i.e., the lowest value) correspond to the solution of the problem. The quantum  
38 annealing process is iterated to the point that an optimal solution, with a sufficient high probability, is  
39 found. The "quantum" in "quantum annealer" refers to the use of multi qubit tunneling [10,11]. The  
40 high degree of parallelism is the advantage of quantum annealing over classical code execution. A  
41 quantum annealer explores all possible inputs in parallel to find the optimal solution to a problem,  
42 which might prove crucial when it comes to solving NP-complete problems. We caution the reader  
43 however that, at present, these techniques should be considered more as an automatic heuristic-finding  
44 program than as a formal solver [13].

45 The preceding facts explain why optimization problems have been associated with quantum  
46 computing principles [14–18]. In this approach, which can be considered as an "analog" method to  
47 tackle optimization problems, the ground state of a Hamiltonian represents an optimal solution of the  
48 optimization problem at hand. Typically, the quantum annealing process starts with the system being  
49 in an equal superposition of all states. Then, an appropriate Hamiltonian is applied and the system  
50 evolves in a time-dependent manner according to the Schrödinger equation. The state of the system  
51 keeps changing according to strength of the local transverse field, which varies with respect to time.  
52 Finally, the transverse field is smoothly turned off and the system finds itself in the ground state of a  
53 properly chosen Hamiltonian that encodes an optimal solution of the optimization problem.

54 After the first commercial launch of an actual system whose functionality is based upon quantum  
55 annealing, the D-Wave platform, it has been demonstrated that these particular quantum machines  
56 are capable of solving certain quadratic unconstrained (mainly binary) optimization problems. The  
57 core of D-Wave's machine that applies the quantum annealing principles for complex combinatorial  
58 optimization problems is the quantum processing unit (QPU). In the D-Wave computer the quantum  
59 bits (which we shall refer to as qubits from now on) are the lowest energy states of superconducting  
60 loops [7,19,20]. In these states there is a circulating current and a corresponding magnetic field. Since a  
61 qubit is a quantum object, its state can be a superposition of the 0 state and the 1 state at the same time.  
62 However, upon measurement a qubit collapses to the state 0 or 1 and behaves like a classical bit. The  
63 quantum annealing process in effect guides the qubits from a superposition of states to their collapse  
64 into either the 0 or 1 state. In the end, the net effect is that the system is in a classical state, which must  
65 encode an (optimal) solution of the problem.

66 The current generation of D-Wave computers employs the Chimera topology. In the Chimera  
67 topology, qubits are sets of connected unit cells, that are connected to four vertical qubits via  
68 couplers [20–22]. The unit cells are oriented vertically and horizontally with adjacent qubits connected,  
69 creating a network of sparsely connected qubits. A Chimera graph consists of an  $N \times N$  grid of unit  
70 cells. The D-Wave 2000Q QPU has up to 2048 qubits which are mapped to a C16 Chimera graph, that is  
71 they are logically mapped into a  $16 \times 16$  matrix of unit cells, each consisting of 8 qubits. In the D-Wave  
72 nomenclature the percentage of working qubits and couplers is known as the working graph, which is  
73 typically a subgraph of the total number of interconnected qubits, which are physically present in the  
74 QPU.

75 A major category of optimization problems, particularly amenable to D-Wave's quantum  
76 annealing, are those that can be expressed as quadratic unconstrained binary optimization (QUBO)  
77 problems. QUBO refers to a pattern matching technique, that, among other applications, can be  
78 used in machine learning and optimization, and which involves minimizing a quadratic polynomial  
79 over binary variables [20,23–29]. We emphasize that QUBO is NP-hard [29]. Some of the most  
80 famous combinatorial optimization problems that can be solved as QUBO problems are the Maximum  
81 Cut, the Graph Coloring and the Partition problem [30]. More details on the QUBO formulation

82 and related results (that are beyond the scope of this paper) can be found in the survey paper of  
83 Kochenberger [25]. QUBO is equivalent to the Ising model, a well-known and extensively studied  
84 model in physics, that was introduced in the mid 1920s by Ernst Ising and Wilhelm Lenz in the field  
85 of ferromagnetism [31,32]. The underlying logical architecture of this model is that variables are  
86 represented as qubits and interactions among qubits stand for the costs associated with each pair of  
87 qubits. In particular, this architecture can be depicted as an undirected graph with qubits as vertices  
88 and couplers as edges among them. The open-source software qbsolv that D-Wave introduced in  
89 2017 is aimed at tackling QUBO problems of higher scale than previous attempts, by utilizing a more  
90 complex graph structure with higher connectivity among QPUs, by partitioning the input into parts  
91 that are then independently solved. This process is repeated using a Tabu-based search until no further  
92 improvement is found [19,33].

93 The literature contains several works that are dedicated to solving the standard TSP or some  
94 relative problem in a quantum setting. One of the first, was the work by Martoňák et al. in [34]  
95 that introduced a different quantum annealing scheme based on path-integral Monte Carlo processes  
96 to address the symmetric version of the Traveling Salesman Problem (sTSP). In [35,36] the D-Wave  
97 platform was used as a test bed for evaluating the efficiency of quantum annealing in solving the  
98 standard TSP compared to classical methods. In [37,38] the well-known variation of the TSP, the  
99 (Capacitated) Vehicle Routing Problem is studied using, again, the D-Wave computer. However, no  
100 work is known to us that tackles the TSP with Time Windows within the QUBO framework, using the  
101 D-Wave platform, or even quantum annealing in general.

102 **Contribution.** In this paper we give the first, to the best of our knowledge, QUBO formulation for  
103 the TSP with Time Windows (TSPTW). The existence of an Ising or QUBO formulation for a problem  
104 is the essential precondition for its solution on the current generation of D-Wave computers. For the  
105 vanilla TSP there exists such a formulation, as presented in an elegant and comprehensive manner  
106 in [32], which has enabled the actual solution of TSP instances on the D-Wave platform (see [35–37]).  
107 In contrast, prior to this work, the TSPTW had not been cast in the QUBO framework. This can be  
108 attributed to the extra difficulty of expressing the time window constraints of TSPTW. We hope and  
109 expect that the formulation presented here will lead to the experimental execution of small-scale  
110 TSPTW instances.

111 This paper is organized as follows. The most relevant to our study work is presented in Section 2.  
112 Section 3 is devoted to the standard definitions and notation of the conventional Traveling Salesman  
113 Problem with Time Windows. Section 4, the most extensive section of this article, contains the main  
114 contribution of our paper. It includes an in-depth presentation of all the required rigorous mathematical  
115 definitions and the proposed modeling that allows us to map the TSPTW into the QUBO framework.  
116 Finally, conclusions and ideas for future work are given in Section 5.

## 117 2. Related work

118 Quantum annealing [5,11] has been shown to provide solutions to a broad range of combinatorial  
119 optimization problems, not only in computer science [6,16,26,30,39–41], but also in other fields, such as  
120 quantum chemistry [42], protein folding [14], vehicle routing [33,38,43,44], etc. This kind of problems  
121 aim at minimizing a cost function, which can be interpreted as finding the ground state of a typical  
122 Ising Hamiltonian [32]. Nevertheless, it is a laborious task to compute a global minimum in problems  
123 where multiple local minima exist [45–47], a fact that shares a lot of similarities to classical spin glasses  
124 [45,46].

125 The possible superiority of quantum computation could be translated into either providing a  
126 better solution (i.e., closest to the optimal one) or arriving at a solution faster or producing a diverse  
127 set of solutions (for the multiobjective case). Some known cases where such methods work well  
128 are spin glasses [48], graph coloring [49], job-shop scheduling [50], machine learning [16,51], graph  
129 partitioning [30], 3-SAT [52], vehicle routing and scheduling [33,38,43,44], neural networks [53], image  
130 processing citecruz2018qubo etc., where the problem parameters can be expressed as boolean variables.

131 Battaglia et al. showed that quantum annealing techniques could outperform their classical  
 132 counterparts on a known NP-complete problem, the 3-SAT, under special circumstances, whereas  
 133 in the general case, the quantum versions did not offer any actual advantage [52]. In a recent work,  
 134 Pagano et al. built a mechanism that implements a shallow-depth quantum approximate optimization  
 135 algorithm (QAOA) by estimating the ground state energy of the Ising model using an analogue  
 136 quantum simulator [54]. Farhi and Harrow tried to show the advantages of quantum approximate  
 137 optimization algorithms compared to classical approaches, providing useful theoretical results and  
 138 bounds, with the emphasis on the idea of “quantum supremacy” than can be established through such  
 139 solutions [55]. Constrained polynomial optimization problems using adiabatic quantum computation  
 140 methods were recently discussed by Reberstrost in [18]. In [56], Venegas-Andraca et al. introduced  
 141 basic algorithms for some well-known problems in combinatorial optimization, like the 3-SAT [52] and  
 142 the max-cut [57] problems. An overview of approaches of the quantum annealing systems used by  
 143 D-Wave Systems [19] is, also, presented.

144 Recently, in [58], Hadfield et al. worked upon the quantum annealing algorithm of Farhi et al. [6],  
 145 extending it by employing the quantum alternating operator ansatz, which yields a broader set of  
 146 operators that can be used by the user. Particularly, this operator allows the representation of a larger  
 147 set of states compared to the original algorithm, aiming to tackle problems with tighter constraints.  
 148 Another work on how to apply constraints in QUBO schemes was presented by Vyskocil and Djidjev  
 149 in [59]. In particular, to avoid the use of large coefficients (hence, more qubits) that result from the use  
 150 of quadratic penalties, they proposed a novel combinatorial design and solving of mixed-integer linear  
 151 programming problems to accommodate the application of the desired constraints.

152 Choi in [7], one of the first studies regarding the commercial D-Wave machine, showed that  
 153 quadratic unconstrained binary optimization (QUBO) problems can be solved using an adiabatic  
 154 quantum computer that employs an Ising spin-1/2 Hamiltonian. This was achieved by the reduction,  
 155 through minor-embedding, of the underlying graph to the quantum hardware graph. The Chimera  
 156 graph is the underlying annealing architecture of the current generation D-Wave platform. Due to  
 157 physical limitations and noise levels, some qubits and couplers cannot be exploited, and are, thus,  
 158 disabled. Therefore, the underlying graph is marginally incomplete [21,22].

159 In a recent technical report, D-Wave systems describe in detail their next generation architecture  
 160 graph, named Pegasus [20]. As claimed by D-Wave itself, Pegasus will offer more flexibility and  
 161 expressiveness over previous topologies, like more efficient embeddings of cliques, penalties, improved  
 162 run times, boosted energy scales, better handling of errors, etc [20]. Similarly, Dattani and Chancellor  
 163 discussed some differences between the two latest quantum annealing architectures from D-Wave  
 164 systems, namely the Chimera and Pegasus graphs [22]. They further proposed a methodology to  
 165 minor embed the required subgraphs on the Chimera and Pegasus graphs.

166 The D-Wave Two, 2X, and 2000Q all used the Chimera graph (see Table 1), which consisted of  
 167 processing unit of  $K_{4,4}$  subgraphs. Each generation of this graph has evolved by exploiting more and  
 168 more qubits (or vertices). On the other hand, Pegasus, the latest graph, totally changed the setting  
 169 by adding more complex connectivity (each qubit or vertex is coupled with 15 other ones) [21]. This  
 170 enhanced connectivity allows for better utilization of the existing qubits, thus fewer vertices are capable  
 171 of broader calculations.

**Table 1.** Evolution of Chimera graphs throughout previous D-Wave versions (from [21]).

	Size of quantum processing unit	Total number of qubits
D-Wave One	$4 \times 4$	128
D-Wave Two	$8 \times 8$	512
D-Wave 2X	$12 \times 12$	1152
D-Wave 2000Q	$16 \times 16$	2048

172 Lucas in [32] discussed Ising formulations for a variety of NP-complete and NP-hard optimization  
173 problems (including the TSP problem), with emphasis on using as few as possible qubits. Martoňák  
174 et al. in [34] introduced a different quantum annealing scheme based on path-integral Monte Carlo  
175 processes to address the symmetric version of the Traveling Salesman Problem (sTSP). Their approach  
176 is built upon a rather constrained Ising-like representation and is compared against the standard  
177 simulated annealing heuristic on various benchmark tests, demonstrating its superiority.

178 Boros et al. presented a set of local search heuristics for Quadratic Unconstrained Binary  
179 Optimization (QUBO) problems, providing indicative simulation results on various benchmark tests  
180 [29]. Adiabatic quantum annealing techniques are also used to address multiobjective optimization  
181 problems. In particular, Barán and Villagra proved their algorithm is capable of finding Pareto-optimal  
182 solutions in finite-time for a particular class of problems [60].

183 Another work on quantum annealing and TSP was presented by Warren in [36]. Warren studied  
184 small-scale instances of traveling salesman problems, showcasing how a D-Wave machine using  
185 quantum annealing would operate to solve these instance. The motivation for this work was to offer  
186 a tutorial-like approach, since the limitations on the number of TSP nodes are quite restrictive for  
187 real-world applications. The mapping of the CMO protein problem to a QUBO formulation was  
188 studied by Oliveira et al. in [61]. Simulation results showed that the proposed approach outperformed  
189 classical techniques.

190 On the other hand, Ushijima-Mwesigwa demonstrated the graph partitioning mechanism of  
191 D-Wave computers utilizing the quantum annealing tools on the D-Wave 2X [30]. The reduction of  
192 the large matrix size in QUBO was the main topic in [24] by Lewis and Glover. This was vital in  
193 order to have a quick solution for large-scale problems with numerous variables that require equally  
194 many qubits. Glover et al. showed in a step by step procedure how one can translate a problem with  
195 particular characteristics into a QUBO instance, using the appropriate tools [28]. Another iterative  
196 version of the quantum annealing heuristic for QUBO problems based on tabu search was presented by  
197 Rosenberg et al. in [62]. Regarding the technical details of that work, their approach tries to partition  
198 the problem into subproblems, while keeping the rest of variables fixed. Moreover, they consider the  
199 effect of the time to reach the best solution on the problems size.

200 Many researchers have studied the classical Traveling Salesman Problem with Time Windows  
201 (TSPTW). The literature can provide exact algorithms for solving the TSPTW. Langevin et al. [63]  
202 introduced a flow formulation of two elements, which can be extended to the classic “makespan”  
203 problem. Dumas et al. [64] used a dynamic programming approach reducing trials, which improved  
204 the performance and scaled down the search space, in advance and during its execution as well. The  
205 TSPTW is an NP-hard problem, since it is a special case of the famous TSP. So, in practice, a heuristic,  
206 which is able to solve effectively realistic cases within a reasonable time, is necessary. Gendreau et  
207 al. [65] proposed an insertion heuristic, which gradually builds the path to the construction phase and  
208 improves a refinement phase. Urrutia et al. [66] proposed a two-stage heuristic, based on VNS. In  
209 the first step, a feasible solution is manufactured using the VNS, wherein the mixed linear, integer,  
210 objective function is represented as an infeasibility measurement. In the second stage, the heuristic  
211 improves the feasible solution with a general version of VNS (General VNS - GVNS).

212 A hybrid genetic algorithm for finding guaranteed and reliable solutions of global optimization  
213 problems using the branch-and-bound technique was proposed by Sotiropoulos et al. [67]. A  
214 branch-and-bound approach was, also, used in the work of Pardalos et al. in [68], where dynamic  
215 preprocessing techniques and heuristics are used to calculate good initial configurations. For an  
216 in-depth insight on quantum genetic algorithms, the reader is referred to the work of Lahoz-Beltra  
217 in [69]).

218 Papalitsas et al. in [70] developed a metaheuristic based on conventional principles for finding  
219 within a short period of time feasible solutions for the TSPTW. Subsequently, a novel quantum-inspired  
220 unconventional metaheuristic method, based on the original General Variable Neighborhood Search  
221 (GVNS), was proposed in order to solve the standard TSP [71]. This quantum inspired metaheuristic

was applied to the solution of the garbage collection problem modeled as a TSP instance [17]. Recently, Papalitsas et al. [72] applied this quantum-inspired metaheuristic to the practical real-life problem of garbage collection with time windows. For the majority of the benchmark instances used to evaluate the proposed metaheuristic, the experimental results were particularly promising. Towards the ultimate goal of running the TSPTW using pure quantum optimization methods, we focus here on its QUBO formulation. This present article is an attempt in that direction.

### 3. The classical formulation of the TSPTW

In this section we give the formal definition of the classical TSPTW. Our presentation follows [73], which is pretty much standard in the relative literature.

**Definition 1.** Let  $G = (N, A)$  be a directed graph, where  $N = \{0, 1, \dots, n\}$  is the finite set of nodes or, more commonly referred to in this context as customers, and  $A = N \times N$  is the set of arcs connecting the customers. For every pair  $(u, v)$  of customers there exists an arc in  $A$ . A tour is defined by the order in which the customers are visited.

A couple of assumptions facilitate the formulation of the TSPTW.

**Definition 2.** Let customer 0 denote the depot and assume that every tour begins and ends at the depot. Each of the remaining  $n$  customers appears exactly once in the tour. We denote a tour as an ordered list  $\mathcal{P} = (p_0, p_1, \dots, p_n, p_{n+1})$ , where  $p_i$  is the index of the customer in the  $i^{\text{th}}$  position of the tour. According to our previous assumption  $p_0 = p_{n+1} = 0$ .

**Definition 3.** For every pair  $(u, v)$  of customers  $u, v \in N$ , there is a cost  $c_{u,v}$ , for traversing the arc  $(u, v)$ . This cost of traversing the arc from  $u$  to  $v$  generally consists of any service time at customer  $U$  plus the travel time from customer  $u$  to customer  $v$ .

**Definition 4.** To each customer  $v \in N$  there is an associated time window  $[e_v, l_v]$ , during which the customer  $v$  must be visited. We assume that waiting is permitted; a vehicle is allowed to reach customer  $v$  before the beginning of its time window,  $e_v$ , but the vehicle cannot depart from customer  $v$  before  $e_v$ .

A tour is feasible if it satisfies the time window of each customer.

In the literature two primary TSPTW objective functions are usually considered

- minimize the sum of the arc traversal costs along the tour, and
- minimize the time to return to the depot.

In a way, the difficulty of the TSPTW stems from the fact that it is two problems in one; a traveling salesman problem and a scheduling problem. The TSP alone is one of the most famous NP-hard optimization problems, while the scheduling part, with release and due dates, adds considerably to the already existing difficulty. To verify that the tour is feasible, i.e., it satisfies the time windows, it is expedient to introduce the **arrival time** at the  $i^{\text{th}}$  customer and the time at which **service** starts at the  $i^{\text{th}}$  customer, which are denoted by  $A_{p_i}$  and  $D_{p_i}$ , respectively. At this point we make the important observation that  $D_{p_i}$  is the **departure time** from the  $i^{\text{th}}$  customer in the case of **zero service time**. The assumption of zero service time is widely used in the literature in order to simplify the problem, and, so, we too shall follow this assumption in our presentation.

The classical formulation of the TSPTW can be summarized by the next relations (see also [73]).

$$\min \sum_{i=1}^{n+1} c_{p_{i-1}, p_i} \quad (1)$$

In the above expression (1), we assume that  $(p_0, p_1, \dots, p_n, p_{n+1})$  is a feasible tour. This means that, besides the assumptions previously outlined, the following hold.

$$D_{p_0} = 0. \quad (2)$$

$$A_{p_i} = D_{p_{i-1}} + c_{p_{i-1}, p_i} \quad (1 \leq i \leq n + 1). \quad (3)$$

$$D_{p_i} = \max\{A_{p_i}, e_{p_i}\} \quad (1 \leq i \leq n). \quad (4)$$

### 262 3.1. An illustrated example for the TSPTW

263 At this subsection we shall describe and explain a template reference problem with 4 nodes plus  
 264 the starting point (5 nodes in total). Although this example is quite simple, we hope that it will help  
 265 the reader to easily understand the TSPTW. Specifically, to better comprehend the modeling of this  
 266 benchmark, as well as the attempt to find a feasible solution at first, and consequently the optimal one.  
 267 The next Figure 1 is the graphical depiction of the 5 customers and all arcs that connect them.

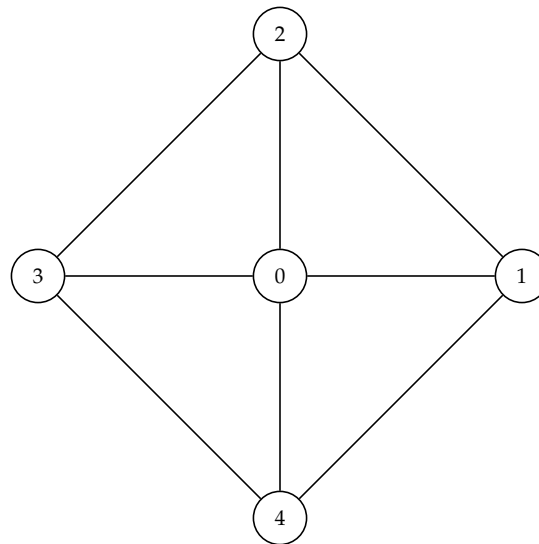


**Figure 1.** The above graph depicts an example of a tour consisting of 4 nodes plus the depot (node 0).

268 Table 2 includes all the relevant data of the above example. In particular, we see the coordinates X  
 269 and Y of every node, as well as the Ready Time and the Due Date.

**Table 2.** The input data for our example.

Node No	X	Y	Ready Time	Due Date
1	2	2	1	30
2	2	3	14	15
3	3	3	12	25
4	3	4	4	5
5	2	1	8	10

270 Table 3 is actually the distance matrix for our example. Let us clarify here that we calculated  
 271 the costs between the nodes using the Euclidean distance, which is given by the well-know formula:  
 272  $d(u, v) = \sqrt{(x_2 - x_1)^2 + (y_2 - y_1)^2}$ , where  $u = (x_1, y_1)$  and  $v = (x_2, y_2)$ .

**Table 3.** The distance matrix.

	Node 1	Node 2	Node 3	Node 4	Node 5
Node 1	0	1	1.41	2.23	1
Node 2	1	0	1	1.41	2
Node3	1.41	1	0	1	2.23
Node 4	2.23	1.41	1	0	3.16
Node 5	1	2	2.23	3.16	0

273 A feasible solution for this particular TSPTW consisting of 5 nodes is given in Table 4. One can  
 274 see that if all time windows are respected in every step of the tour going from from one customer to  
 275 the next, a feasible solution can be constructed. Although, this is a small scale example, we expect that  
 276 it will enhance one's understanding of what is a feasible solution for the TSPTW.

**Table 4.** A feasible solution of our illustrated example.

Ordering	Node 1	Node 4	Node 5	Node 3	Node 2
cost	0<1	2.23 <4	7.16 <8	10 <12	12<14
feasibility	yes	yes	yes	yes	yes

277 In the next section we introduce our novel approach for mapping the TSPTW over the quadratic  
 278 unconstrained binary optimization (QUBO) model.

#### 279 4. A QUBO formulation for the TSPTW

280 In the literature, the typical QUBO formulation of the standard TSP involves the use of a set of  
 281 *binary* variables (see [32]). They are characterized as binary in the sense that they can take only the 0 or  
 282 1 value. Typically, they are denoted by  $x_{v,i}$ , and their meaning is the following:

$$x_{v,i} = \begin{cases} 1, & \text{customer } v \text{ is at position } i \text{ in the tour} \\ 0, & \text{otherwise} \end{cases} \quad (5)$$

283 In the case of the TSPTW, we have discovered to be more advantageous to use binary variables  
 284 parameterized by three integers:  $u, v$  and  $i$ . A similar suggestion for the Vehicle Routing Problem can  
 285 be found in [38]. Hence, in the rest of our analysis, we shall use the binary variables  $x_{u,v}^i$  defined next:

$$x_{u,v}^i = \begin{cases} 1, & \text{customers } u \text{ and } v \text{ are at consecutive positions } i-1 \text{ and } i \text{ in the tour} \\ 0, & \text{otherwise} \end{cases} \quad (6)$$

286 As we explained in the previous section, a feasible tour has the form  $\{p_0, p_1, \dots, p_n, p_{n+1}\}$ . In  
 287 this enumeration,  $p_i$  is the customer in the  $i^{\text{th}}$  position of the tour. We always take for granted that  
 288  $p_0 = p_{n+1} = 0$  and each other customer appears exactly once. We recall the assumption of *zero service*  
 289 *time* at each customer, and without loss of generality, we adopt another assumption that greatly reduces  
 290 the final clutter of our QUBO expressions: for each customer  $v$ , where  $0 \leq v \leq n+1$ ,  $e_v = 0$ . With this  
 291 understanding, we see that the parameters  $u$  and  $v$  range from 0 to  $n$  and the parameter  $i$  ranges from  
 292 1 to  $n+1$ .

293 Therefore, we can assert that:

- 294 • For each  $i$ ,  $1 \leq i \leq n+1$ , exactly one of the binary variables  $x_{u,v}^i$  is 1, where  $u$  and  $v$  range freely  
 295 from 0 to  $n$ , with the proviso that  $u \neq v$ . As a matter of fact when  $i = 1$  and  $i = n+1$  we can  
 296 be more precise. In the former case, exactly one of the binary variables  $x_{0,v}^1$  is 1, where  $v$  ranges  
 297 from 1 to  $n$ , and, in the latter case, exactly one of the binary variables  $x_{v,0}^{n+1}$  is 1, where  $v$  ranges  
 298 from 1 to  $n$ .



- 299 • In addition to the above constraints, for each  $u$ ,  $1 \leq u \leq n$ , exactly one of the binary variables  
 300  $x_{u,v}^i$  is 1, where  $i$  ranges from 2 to  $n$  and  $v$  ranges from 1 to  $n$ .  
 301 • Symmetrically, we also have the constraint that for every  $v$ ,  $1 \leq v \leq n$ , exactly one of the binary  
 302 variables  $x_{u,v}^i$  is 1, where  $i$  ranges from 2 to  $n$  and  $u$  ranges from 1 to  $n$ .

303 These constraints are encoded in the Hamiltonian  $H_c$ .

$$\begin{aligned}
 H_c = & B \sum_{i=1}^{n+1} \left( 1 - \sum_{u=0}^n \sum_{\substack{v=0 \\ v \neq u}}^n x_{u,v}^i \right)^2 + B \left( 1 - \sum_{v=1}^n x_{0,v}^1 \right)^2 + B \left( 1 - \sum_{v=1}^n x_{v,0}^{n+1} \right)^2 \\
 & + B \sum_{u=1}^n \left( 1 - \sum_{i=2}^n \sum_{v=1}^n x_{u,v}^i \right)^2 \\
 & + B \sum_{v=1}^n \left( 1 - \sum_{i=2}^n \sum_{u=1}^n x_{u,v}^i \right)^2
 \end{aligned} \tag{7}$$

304 Using the  $x_{u,v}^i$  binary variables, the requirement that the tour be minimal can be encoded by the  
 305 following Hamiltonian  $H_m$ .

$$H_m = C \sum_{i=1}^{n+1} \sum_{u=0}^n \sum_{\substack{v=0 \\ v \neq u}}^n x_{u,v}^i c_{u,v} . \tag{8}$$

306 In the above Hamiltonians,  $B$  and  $C$  are positive constants, which must be appropriately chosen,  
 307 i.e.,  $C < B$ , so as to ensure that the constraints of  $H_c$  are respected (see also [32]). Obviously,  $c_{u,v}$  is the  
 308 cost for traversing the arc  $(u, v)$ .

309 The above Hamiltonians are certainly not the end of the story in the case of the TSPTW, as, in their  
 310 essence, they just encode the minimal cost of the Hamiltonian circuit. There are a lot more difficult  
 311 time constraints to tackle in order to satisfy the time window of every customer. To this end, besides  
 312 the binary variables  $x_{u,v}^i$ , it will be necessary to use a second type of binary variables, denoted by  $t_{n,i}$ ,  
 313 in order to express the *time margin* of every customer.

314 **Definition 5.** Given a feasible tour  $p_0, p_1, \dots, p_n, p_{n+1}$ , suppose that the customer at position  $i$ , where  
 315  $1 \leq i \leq n$ , is  $v$  with time window  $[e_v, l_v]$ . We say that the *time margin* of the customer at position  $i$  to be  
 316  $l_v - A_{p_i}$ .

317 Clearly, for a feasible tour, the time margin for every position of the tour is non negative. We can  
 318 now define the binary variables  $t_{k,i}$  as follows:

$$t_{k,i} = \begin{cases} 1, & \text{the time margin of the customer at position } i \text{ in the tour is } k \\ 0, & \text{otherwise} \end{cases} . \tag{9}$$

319 We recall that in the formulation of the TSPTW, the arrival time at the customer in the  $i^{\text{th}}$  position  
 320 of the tour, denoted  $A_{p_i}$ , plays an important role (see [73]). Thus, we begin our analysis by showing  
 321 how to express  $A_{p_i}$ . Obviously,  $A_{p_0} = 0$ , so it is only necessary to give the formula for  $A_{p_i}$ ,  $1 \leq i \leq n$ .  
 322 We first observe that the customer at position 0 is always the depot (customer 0), which results in the  
 323 following, relatively simple formula, for  $A_{p_1}$ .

$$A_{p_1} = \sum_{v=1}^n x_{0,v}^1 c_{0,v} . \tag{10}$$

324 The general case, i.e., when  $2 \leq i \leq n$ , is taken care by the next equation.

$$A_{p_i} = \sum_{d=1}^i \sum_{u=1}^n \sum_{\substack{v=1 \\ v \neq u}}^n x_{u,v}^d c_{u,v} \quad (2 \leq i \leq n). \quad (11)$$

325 **Example 1.** To explain how Equations (10) and (11) can be used in practice, we continue with our test case  
 326 example.

327 Equation (10) becomes

$$A_{p_1} = x_{0,1}^1 c_{0,1} + x_{0,2}^1 c_{0,2} + x_{0,3}^1 c_{0,3} + x_{0,4}^1 c_{0,4} \quad (12)$$

328 Equation (11) gives the following series of equations.

$$A_{p_2} = \left( \underbrace{x_{0,1}^1 c_{0,1} + x_{0,2}^1 c_{0,2} + x_{0,3}^1 c_{0,3} + x_{0,4}^1 c_{0,4}}_{A_{p_1}} \right) + x_{1,2}^2 c_{1,2} + x_{1,3}^2 c_{1,3} + x_{1,4}^2 c_{1,4} + x_{2,1}^2 c_{2,1} + x_{2,3}^2 c_{2,3} + x_{2,4}^2 c_{2,4} + x_{3,1}^2 c_{3,1} + x_{3,2}^2 c_{3,2} + x_{3,4}^2 c_{3,4} + x_{4,1}^2 c_{4,1} + x_{4,2}^2 c_{4,2} + x_{4,3}^2 c_{4,3} \quad (13)$$

$$A_{p_3} = \left( \left( x_{0,1}^1 c_{0,1} + x_{0,2}^1 c_{0,2} + x_{0,3}^1 c_{0,3} + x_{0,4}^1 c_{0,4} \right) + x_{1,2}^2 c_{1,2} + x_{1,3}^2 c_{1,3} + x_{1,4}^2 c_{1,4} + x_{2,1}^2 c_{2,1} + x_{2,3}^2 c_{2,3} + x_{2,4}^2 c_{2,4} + x_{3,1}^2 c_{3,1} + x_{3,2}^2 c_{3,2} + x_{3,4}^2 c_{3,4} + x_{4,1}^2 c_{4,1} + x_{4,2}^2 c_{4,2} + x_{4,3}^2 c_{4,3} \right) + x_{1,2}^3 c_{1,2} + x_{1,3}^3 c_{1,3} + x_{1,4}^3 c_{1,4} + x_{2,1}^3 c_{2,1} + x_{2,3}^3 c_{2,3} + x_{2,4}^3 c_{2,4} + x_{3,1}^3 c_{3,1} + x_{3,2}^3 c_{3,2} + x_{3,4}^3 c_{3,4} + x_{4,1}^3 c_{4,1} + x_{4,2}^3 c_{4,2} + x_{4,3}^3 c_{4,3} \quad (14)$$

$$A_{p_4} = x_{0,1}^1 c_{0,1} + x_{0,2}^1 c_{0,2} + x_{0,3}^1 c_{0,3} + x_{0,4}^1 c_{0,4} + x_{1,2}^2 c_{1,2} + x_{1,3}^2 c_{1,3} + x_{1,4}^2 c_{1,4} + x_{2,1}^2 c_{2,1} + x_{2,3}^2 c_{2,3} + x_{2,4}^2 c_{2,4} + x_{3,1}^2 c_{3,1} + x_{3,2}^2 c_{3,2} + x_{3,4}^2 c_{3,4} + x_{4,1}^2 c_{4,1} + x_{4,2}^2 c_{4,2} + x_{4,3}^2 c_{4,3} + x_{1,2}^3 c_{1,2} + x_{1,3}^3 c_{1,3} + x_{1,4}^3 c_{1,4} + x_{2,1}^3 c_{2,1} + x_{2,3}^3 c_{2,3} + x_{2,4}^3 c_{2,4} + x_{3,1}^3 c_{3,1} + x_{3,2}^3 c_{3,2} + x_{3,4}^3 c_{3,4} + x_{4,1}^3 c_{4,1} + x_{4,2}^3 c_{4,2} + x_{4,3}^3 c_{4,3} + x_{1,2}^4 c_{1,2} + x_{1,3}^4 c_{1,3} + x_{1,4}^4 c_{1,4} + x_{2,1}^4 c_{2,1} + x_{2,3}^4 c_{2,3} + x_{2,4}^4 c_{2,4} + x_{3,1}^4 c_{3,1} + x_{3,2}^4 c_{3,2} + x_{3,4}^4 c_{3,4} + x_{4,1}^4 c_{4,1} + x_{4,2}^4 c_{4,2} + x_{4,3}^4 c_{4,3} \quad (15)$$

329 The above equations demonstrate that in every case,  $A_{p_i}$  can be expressed as a sum of terms, where each  
 330 term is the product of an input variable  $c_{u,v}$  and exactly one binary decision variable  $x_{u,v}^i$ .

331 The simplifying assumption of zero service time enables us to express the constraints imposed by  
 332 the time windows of every customer as follows:

$$A_{p_1} \leq \sum_{v=1}^n x_{0,v}^1 l_v, \quad (16)$$

for the special case where  $i = 1$ , and

$$A_{p_i} \leq \sum_{u=1}^n \sum_{\substack{v=1 \\ v \neq u}}^n x_{u,v}^i l_v \quad (2 \leq i \leq n), \quad (17)$$

333 for the general case where  $2 \leq i \leq n$ .

334 The above expression may seem a little complicated, but, unfortunately, while  $A_{p_i}$  tells us the  
335 arrival time at the customer in the  $i^{\text{th}}$  position of the tour, it does not tell us *which* is this particular  
336 customer. We have to resort to the binary variables  $x_{u,v}^i$  to indirectly obtain this information.

337 Inequality constraints such as these in (16) and (17) are notoriously difficult to express within the  
338 QUBO framework. For an extensive analysis we refer the interested reader to [28,59,74]. The approach  
339 which is most commonly used in the literature is to employ auxiliary binary variables, like the binary  
340 variables  $t_{k,i}$  previously defined, to convert the inequality into an equality, and then proceed, as usual,  
341 by squaring the equality constraint.

342 In our case, the first step is to express the inequalities (16) and (17) as

$$A_{p_1} + \sum_{k=1}^K kt_{k,1} = \sum_{v=1}^n x_{0,v}^1 l_v, \quad (18)$$

and as

$$A_{p_i} + \sum_{k=1}^K kt_{k,i} = \sum_{u=1}^n \sum_{\substack{v=1 \\ v \neq u}}^n x_{u,v}^i l_v \quad (2 \leq i \leq n), \quad (19)$$

343 respectively.

344 In the above equalities  $K$  is a positive constant appropriately chosen taking into consideration  
345 the specific time windows. A valid possible choice could be  $K = \max_{1 \leq v \leq n} \{l_v\}$ . Such a choice, while  
346 valid, would be unnecessarily big in most practical cases.

347 Equality constraints like (18) and (19) are typically treated in QUBO by converting them into  
348 squared expressions. Hence, (18) gives rise to the first time window constraint, denoted by  $W_1$  and  
349 given by

$$W_1 = \left( A_{p_1} + \sum_{k=1}^K kt_{k,1} - \sum_{v=1}^n x_{0,v}^1 l_v \right)^2, \quad (20)$$

while Equation (19) gives rise to the  $i^{\text{th}}$  time window constraint, denoted by  $W_i$  and given by:

$$W_i = \left( A_{p_i} + \sum_{k=1}^K kt_{k,i} - \sum_{u=1}^n \sum_{\substack{v=1 \\ v \neq u}}^n x_{u,v}^i l_v \right)^2 \quad (2 \leq i \leq n). \quad (21)$$

350 If we replace  $A_{p_1}$  and  $A_{p_i}$  in the above equations by the formulas in (10) and (11), we derive the  
351 expanded forms of  $W_1$  and  $W_i$ ,  $2 \leq i \leq n$ , respectively.

$$W_1 = \left( \sum_{v=1}^n x_{0,v}^1 c_{0,v} + \sum_{k=1}^K kt_{k,1} - \sum_{v=1}^n x_{0,v}^1 l_v \right)^2. \quad (22)$$

$$W_i = \left( \sum_{d=1}^i \sum_{u=1}^n \sum_{\substack{v=1 \\ v \neq u}}^n x_{u,v}^d c_{u,v} + \sum_{k=1}^K kt_{k,i} - \sum_{u=1}^n \sum_{\substack{v=1 \\ v \neq u}}^n x_{u,v}^i l_v \right)^2 \quad (2 \leq i \leq n). \quad (23)$$

At this point it is important to pause and confirm that the constraints in Equations (22) and (23) conform to the QUBO formulation requirements, in the sense that, after the expansion of the square, we get a sum of terms, where each term is the product of input data like  $c_{u,v}$  or  $l_v$  and *at most two* binary decision variables.

The last time constraint concerns the binary variables  $t_{k,i}$ . For each  $i$ ,  $1 \leq i \leq n$ , exactly one of the binary variables  $t_{k,i}$  is 1, where  $k$  ranges from 1 to  $K$ . The meaning of this constraint is obvious: in every position of a feasible tour the time margin should be unique. Expressing this constraint is also straightforward:

$$M_i = \left( 1 - \sum_{k=1}^K t_{k,i} \right)^2 \quad (1 \leq i \leq n). \quad (24)$$

Putting all the time constraints together results in the Hamiltonian  $H_t$ :

$$H_t = T(W_1) + T \sum_{i=2}^n TWC_i + T \sum_{i=1}^n M_i. \quad (25)$$

Therefore, to solve the TSPTW in the QUBO framework we must use the Hamiltonian  $H$  given below:

$$H = H_c + H_m + H_t. \quad (26)$$

As noted earlier, the constants  $B$ ,  $C$  and  $T$  appearing in the Hamiltonians are positive constants, which must be chosen according to our requirements. For instance, by setting  $C < B$ , so as to ensure that the constraints of  $H_c$  are respected; similarly, setting  $T < B$  prioritizes the time windows constraints over the minimality of the tour.

**Example 2.** To show the form of the time windows constraints when the square is expanded, we apply constraint (22) to our test case example.

First we point out that for binary variables the following hold:

$$(x_{u,v}^i)^2 = x_{u,v}^i \quad \text{and} \quad (t_{k,i})^2 = t_{k,i}. \quad (27)$$

We also recall the identity:  $(a + b - c)^2 = a^2 + b^2 + c^2 + 2ab - 2ac - 2bc$ . We shall use this identity to expand (22), setting  $a = \sum_{v=1}^n x_{0,v}^1 c_{0,v}$ ,  $b = \sum_{k=1}^K kt_{k,1}$ , and  $c = \sum_{v=1}^n x_{0,v}^1 l_v$ . In our example  $n = 4$  and, in order to simplify somewhat the calculations we take  $K = 2$ . With this understanding we use Equation (12) to derive the formulas given below. Note that to improve the readability of the equations in this example, we have written in green color those terms that involve exactly one binary variable and in blue color those terms that involve exactly two binary variables.

$$\begin{aligned}
A_{p_1}^2 &= \left( x_{0,1}^1 c_{0,1} + x_{0,2}^1 c_{0,2} + x_{0,3}^1 c_{0,3} + x_{0,4}^1 c_{0,4} \right)^2 \\
&= (x_{0,1}^1)^2 c_{0,1}^2 + (x_{0,2}^1)^2 c_{0,2}^2 + (x_{0,3}^1)^2 c_{0,3}^2 + (x_{0,4}^1)^2 c_{0,4}^2 + 2x_{0,1}^1 c_{0,1} x_{0,2}^1 c_{0,2} + 2x_{0,1}^1 c_{0,1} x_{0,3}^1 c_{0,3} \\
&\quad + 2x_{0,1}^1 c_{0,1} x_{0,4}^1 c_{0,4} + 2x_{0,2}^1 c_{0,2} x_{0,3}^1 c_{0,3} + 2x_{0,2}^1 c_{0,2} x_{0,4}^1 c_{0,4} + 2x_{0,3}^1 c_{0,3} x_{0,4}^1 c_{0,4} \\
&= x_{0,1}^1 c_{0,1}^2 + x_{0,2}^1 c_{0,2}^2 + x_{0,3}^1 c_{0,3}^2 + x_{0,4}^1 c_{0,4}^2 + 2x_{0,1}^1 c_{0,1} x_{0,2}^1 c_{0,2} + 2x_{0,1}^1 c_{0,1} x_{0,3}^1 c_{0,3} \\
&\quad + 2x_{0,1}^1 c_{0,1} x_{0,4}^1 c_{0,4} + 2x_{0,2}^1 c_{0,2} x_{0,3}^1 c_{0,3} + 2x_{0,2}^1 c_{0,2} x_{0,4}^1 c_{0,4} + 2x_{0,3}^1 c_{0,3} x_{0,4}^1 c_{0,4}
\end{aligned} \tag{28}$$

376

Similarly, we see that:

$$\left( \sum_{k=1}^2 kt_{k,1} \right)^2 = (1t_{1,1} + 2t_{2,1})^2 = t_{1,1}^2 + 4t_{2,1}^2 + 4t_{1,1}t_{2,1} = t_{1,1} + 4t_{2,1} + 4t_{1,1}t_{2,1} \tag{29}$$

$$\begin{aligned}
\left( \sum_{v=1}^4 x_{0,v}^1 l_v \right)^2 &= \left( x_{0,1}^1 l_1 + x_{0,2}^1 l_2 + x_{0,3}^1 l_3 + x_{0,4}^1 l_4 \right)^2 \\
&= (x_{0,1}^1)^2 l_1^2 + (x_{0,2}^1)^2 l_2^2 + (x_{0,3}^1)^2 l_3^2 + (x_{0,4}^1)^2 l_4^2 + 2x_{0,1}^1 l_1 x_{0,2}^1 l_2 + 2x_{0,1}^1 l_1 x_{0,3}^1 l_3 \\
&\quad + 2x_{0,1}^1 l_1 x_{0,4}^1 l_4 + 2x_{0,2}^1 l_2 x_{0,3}^1 l_3 + 2x_{0,2}^1 l_2 x_{0,4}^1 l_4 + 2x_{0,3}^1 l_3 x_{0,4}^1 l_4 \\
&= x_{0,1}^1 l_1^2 + x_{0,2}^1 l_2^2 + x_{0,3}^1 l_3^2 + x_{0,4}^1 l_4^2 + 2x_{0,1}^1 l_1 x_{0,2}^1 l_2 + 2x_{0,1}^1 l_1 x_{0,3}^1 l_3 \\
&\quad + 2x_{0,1}^1 l_1 x_{0,4}^1 l_4 + 2x_{0,2}^1 l_2 x_{0,3}^1 l_3 + 2x_{0,2}^1 l_2 x_{0,4}^1 l_4 + 2x_{0,3}^1 l_3 x_{0,4}^1 l_4
\end{aligned} \tag{30}$$

$$\begin{aligned}
2A_{p_1} \sum_{k=1}^2 kt_{k,1} &= 2 \left( x_{0,1}^1 c_{0,1} + x_{0,2}^1 c_{0,2} + x_{0,3}^1 c_{0,3} + x_{0,4}^1 c_{0,4} \right) (1t_{1,1} + 2t_{2,1}) \\
&= 2x_{0,1}^1 c_{0,1} t_{1,1} + 2x_{0,1}^1 c_{0,1} t_{2,1} + 2x_{0,2}^1 c_{0,2} t_{1,1} + 2x_{0,2}^1 c_{0,2} t_{2,1} \\
&\quad + 2x_{0,3}^1 c_{0,3} t_{1,1} + 2x_{0,3}^1 c_{0,3} t_{2,1} + 2x_{0,4}^1 c_{0,4} t_{1,1} + 2x_{0,4}^1 c_{0,4} t_{2,1}
\end{aligned} \tag{31}$$

$$\begin{aligned}
2A_{p_1} \sum_{v=1}^4 x_{0,v}^1 l_v &= 2 \left( x_{0,1}^1 c_{0,1} + x_{0,2}^1 c_{0,2} + x_{0,3}^1 c_{0,3} + x_{0,4}^1 c_{0,4} \right) \left( x_{0,1}^1 l_1 + x_{0,2}^1 l_2 + x_{0,3}^1 l_3 + x_{0,4}^1 l_4 \right) \\
&= 2(x_{0,1}^1)^2 c_{0,1} l_1 + 2x_{0,1}^1 c_{0,1} x_{0,2}^1 l_2 + 2x_{0,1}^1 c_{0,1} x_{0,3}^1 l_3 + 2x_{0,1}^1 c_{0,1} x_{0,4}^1 l_4 \\
&\quad + 2x_{0,2}^1 c_{0,2} x_{0,1}^1 l_1 + 2(x_{0,2}^1)^2 c_{0,2} l_2 + 2x_{0,2}^1 c_{0,2} x_{0,3}^1 l_3 + 2x_{0,2}^1 c_{0,2} x_{0,4}^1 l_4 \\
&\quad + 2x_{0,3}^1 c_{0,3} x_{0,1}^1 l_1 + 2x_{0,3}^1 c_{0,3} x_{0,2}^1 l_2 + 2(x_{0,3}^1)^2 c_{0,3} l_3 + 2x_{0,3}^1 c_{0,3} x_{0,4}^1 l_4 \\
&\quad + 2x_{0,4}^1 c_{0,4} x_{0,1}^1 l_1 + 2x_{0,4}^1 c_{0,4} x_{0,2}^1 l_2 + 2x_{0,4}^1 c_{0,4} x_{0,3}^1 l_3 + 2(x_{0,4}^1)^2 c_{0,4} l_4 \\
&= 2x_{0,1}^1 c_{0,1} l_1 + 2x_{0,2}^1 c_{0,2} l_2 + 2x_{0,3}^1 c_{0,3} l_3 + 2x_{0,4}^1 c_{0,4} l_4 \\
&\quad + 2x_{0,1}^1 c_{0,1} x_{0,2}^1 l_2 + 2x_{0,1}^1 c_{0,1} x_{0,3}^1 l_3 + 2x_{0,1}^1 c_{0,1} x_{0,4}^1 l_4 \\
&\quad + 2x_{0,2}^1 c_{0,2} x_{0,1}^1 l_1 + 2x_{0,2}^1 c_{0,2} x_{0,3}^1 l_3 + 2x_{0,2}^1 c_{0,2} x_{0,4}^1 l_4 \\
&\quad + 2x_{0,3}^1 c_{0,3} x_{0,1}^1 l_1 + 2x_{0,3}^1 c_{0,3} x_{0,2}^1 l_2 + 2x_{0,3}^1 c_{0,3} x_{0,4}^1 l_4 \\
&\quad + 2x_{0,4}^1 c_{0,4} x_{0,1}^1 l_1 + 2x_{0,4}^1 c_{0,4} x_{0,2}^1 l_2 + 2x_{0,4}^1 c_{0,4} x_{0,3}^1 l_3
\end{aligned} \tag{32}$$

$$\begin{aligned}
2 \sum_{k=1}^2 kt_{k,1} \sum_{v=1}^4 x_{0,v}^1 l_v &= 2 (t_{1,1} + 2t_{2,1}) (x_{0,1}^1 l_1 + x_{0,2}^1 l_2 + x_{0,3}^1 l_3 + x_{0,4}^1 l_4) \\
&= 2t_{1,1} x_{0,1}^1 l_1 + 2t_{1,1} x_{0,2}^1 l_2 + 2t_{1,1} x_{0,3}^1 l_3 + 2t_{1,1} x_{0,4}^1 l_4 \\
&\quad + 4t_{2,1} x_{0,1}^1 l_1 + 4t_{2,1} x_{0,2}^1 l_2 + 4t_{2,1} x_{0,3}^1 l_3 + 4t_{2,1} x_{0,4}^1 l_4
\end{aligned} \tag{33}$$

377 We can now substitute Equations (28)–(33) in (22) to finally arrive at the expanded form of the constraint,  
378 given by the following equation.

$$\begin{aligned}
W_1 &= x_{0,1}^1 c_{0,1}^2 + x_{0,2}^1 c_{0,2}^2 + x_{0,3}^1 c_{0,3}^2 + x_{0,4}^1 c_{0,4}^2 + 2x_{0,1}^1 c_{0,1} x_{0,2}^1 c_{0,2} + 2x_{0,1}^1 c_{0,1} x_{0,3}^1 c_{0,3} \\
&\quad + 2x_{0,1}^1 c_{0,1} x_{0,4}^1 c_{0,4} + 2x_{0,2}^1 c_{0,2} x_{0,3}^1 c_{0,3} + 2x_{0,2}^1 c_{0,2} x_{0,4}^1 c_{0,4} + 2x_{0,3}^1 c_{0,3} x_{0,4}^1 c_{0,4} \\
&\quad + t_{1,1} + 4t_{2,1} + 4t_{1,1} t_{2,1} \\
&\quad + x_{0,1}^1 l_1^2 + x_{0,2}^1 l_2^2 + x_{0,3}^1 l_3^2 + x_{0,4}^1 l_4^2 + 2x_{0,1}^1 l_1 x_{0,2}^1 l_2 + 2x_{0,1}^1 l_1 x_{0,3}^1 l_3 \\
&\quad + 2x_{0,1}^1 l_1 x_{0,4}^1 l_4 + 2x_{0,2}^1 l_2 x_{0,3}^1 l_3 + 2x_{0,2}^1 l_2 x_{0,4}^1 l_4 + 2x_{0,3}^1 l_3 x_{0,4}^1 l_4 \\
&\quad - 2x_{0,1}^1 c_{0,1} t_{1,1} - 2x_{0,1}^1 c_{0,1} t_{2,1} - 2x_{0,2}^1 c_{0,2} t_{1,1} - 2x_{0,2}^1 c_{0,2} t_{2,1} \\
&\quad - 2x_{0,3}^1 c_{0,3} t_{1,1} - 2x_{0,3}^1 c_{0,3} t_{2,1} - 2x_{0,4}^1 c_{0,4} t_{1,1} - 2x_{0,4}^1 c_{0,4} t_{2,1} \\
&\quad - 2x_{0,1}^1 c_{0,1} l_1 - 2x_{0,2}^1 c_{0,2} l_2 - 2x_{0,3}^1 c_{0,3} l_3 - 2x_{0,4}^1 c_{0,4} l_4 \\
&\quad - 2x_{0,1}^1 c_{0,1} x_{0,2}^1 l_2 - 2x_{0,1}^1 c_{0,1} x_{0,3}^1 l_3 - 2x_{0,1}^1 c_{0,1} x_{0,4}^1 l_4 \\
&\quad - 2x_{0,2}^1 c_{0,2} x_{0,1}^1 l_1 - 2x_{0,2}^1 c_{0,2} x_{0,3}^1 l_3 - 2x_{0,2}^1 c_{0,2} x_{0,4}^1 l_4 \\
&\quad - 2x_{0,3}^1 c_{0,3} x_{0,1}^1 l_1 - 2x_{0,3}^1 c_{0,3} x_{0,2}^1 l_2 - 2x_{0,3}^1 c_{0,3} x_{0,4}^1 l_4 \\
&\quad - 2x_{0,4}^1 c_{0,4} x_{0,1}^1 l_1 - 2x_{0,4}^1 c_{0,4} x_{0,2}^1 l_2 - 2x_{0,4}^1 c_{0,4} x_{0,3}^1 l_3 \\
&\quad - 2t_{1,1} x_{0,1}^1 l_1 - 2t_{1,1} x_{0,2}^1 l_2 - 2t_{1,1} x_{0,3}^1 l_3 - 2t_{1,1} x_{0,4}^1 l_4 \\
&\quad - 4t_{2,1} x_{0,1}^1 l_1 - 4t_{2,1} x_{0,2}^1 l_2 - 4t_{2,1} x_{0,3}^1 l_3 - 4t_{2,1} x_{0,4}^1 l_4
\end{aligned} \tag{34}$$

379 Similar calculations, albeit too lengthy to include here, confirm that all time window constraints have  
380 similar patterns, that is they constitute legitimate expressions within the QUBO framework.

## 381 5. Conclusions and future work

382 In this work, we have considered the TSPTW. Although many combinatorial optimization  
383 problems have been expressed in the QUBO (or, equivalently, the Ising) formulation, this particular  
384 problem was not one of them. Presumably, the reason is the TSPTW imposes many additional (time)  
385 constraints because the customers' time windows must be satisfied. These are actually inequality  
386 constraints that are very difficult to tackle within the QUBO framework. We remind the reader that  
387 valid QUBO expressions must have the form:  $x^T Q x$ , where  $x$  is a column vector of binary decision  
388 variables,  $x^T$  its transpose and  $Q$  a square matrix of constants. So, to the best of our knowledge, this is  
389 the first time the TSPTW is cast in QUBO form.

390 This step is a necessary precondition in order to be able to run TSPTW instances on the current  
391 generation of D-Wave computers. Hence, the future direction of this work will be the mapping of TSPTW  
392 benchmarks to the Chimera or the upcoming Pegasus architecture, so as to obtain experimental results.  
393 This will enable the comparison of the current state of the art classical, or conventional, if you prefer,  
394 metaheuristics with the purely quantum approach. This comparison is expected to shed some light on  
395 the pressing question of whether quantum annealing is more efficient than classical methods, and, if  
396 so, to what degree.

397 **Author Contributions:** Conceptualization, Christos Papalitsas and Theodore Andronikos; Formal  
398 analysis, Christos Papalitsas and Theodore Andronikos; Methodology, Christos Papalitsas and Theodore

399 Andronikos; Supervision, Theodore Andronikos; Validation, Christos Papalitsas and Sofia Fanarioti; Writing -  
 400 original draft, Konstantinos Giannakis and Georgia Theocharopoulou; Writing - review & editing, Konstantinos  
 401 Giannakis, Georgia Theocharopoulou, Christos Papalitsas, Sofia Fanarioti and Theodore Andronikos.

402 **Funding:** This research is funded in the context of the project “Investigating alternative computational methods  
 403 and their use in computational problems related to optimization and game theory,” (MIS 5007500) under the  
 404 call for proposals “Supporting researchers with an emphasis on young researchers” (EDULL34). The project is  
 405 co-financed by Greece and the European Union (European Social Fund - ESF) by the Operational Programme  
 406 Human Resources Development, Education and Lifelong Learning 2014-2020.

407 **Conflicts of Interest:** The authors declare no conflicts of interest.

## 408 Abbreviations

409 The following abbreviations are used in this manuscript:

410	QPU	Quantum Processing Unit
	QUBO	Quadratic Unconstrained Binary Optimization
411	TSP	Traveling Salesman Problem
	TSPTW	Traveling Salesman Problem with Time Windows

412

- 413 1. Feynman, R.P. Simulating physics with computers. *International Journal of Theoretical Physics Int J Theor*  
 414 *Phys* **1982**, *21*, 467–488.
- 415 2. Shor, P.W. Polynomial-time algorithms for prime factorization and discrete logarithms on a quantum  
 416 computer. *SIAM review* **1999**, *41*, 303–332.
- 417 3. Grover, L. A fast quantum mechanical algorithm for database search. Proc. of the Twenty-Eighth Annual  
 418 ACM Symposium on the Theory of Computing, 1996, 1996.
- 419 4. Nielsen, M.A.; Chuang, I.L. *Quantum computation and quantum information*; Cambridge university press,  
 420 2010.
- 421 5. Farhi, E.; Goldstone, J.; Gutmann, S.; Sipsers, M. Quantum computation by adiabatic evolution. *arXiv*  
 422 *preprint quant-ph/0001106* **2000**.
- 423 6. Farhi, E.; Goldstone, J.; Gutmann, S.; Lapan, J.; Lundgren, A.; Preda, D. A quantum adiabatic evolution  
 424 algorithm applied to random instances of an NP-complete problem. *Science* **2001**, *292*, 472–475.
- 425 7. Choi, V. Minor-embedding in adiabatic quantum computation: I. The parameter setting problem. *Quantum*  
 426 *Information Processing* **2008**, *7*, 193–209.
- 427 8. Messiah, A. *Quantum mechanics*, 1961.
- 428 9. Amin, M. Consistency of the adiabatic theorem. *Physical review letters* **2009**, *102*, 220401.
- 429 10. Kadowaki, T. Study of optimization problems by quantum annealing. *arXiv preprint quant-ph/0205020*  
 430 **2002**.
- 431 11. Kadowaki, T.; Nishimori, H. Quantum annealing in the transverse Ising model. *Physical Review E* **1998**,  
 432 *58*, 5355.
- 433 12. Kirkpatrick, S.; Gelatt, C.D.; Vecchi, M.P. Optimization by simulated annealing. *science* **1983**, *220*, 671–680.
- 434 13. Pakin, S. Performing fully parallel constraint logic programming on a quantum annealer. *Theory and*  
 435 *Practice of Logic Programming* **2018**, *18*, 928–949.
- 436 14. Perdomo-Ortiz, A.; Dickson, N.; Drew-Brook, M.; Rose, G.; Aspuru-Guzik, A. Finding low-energy  
 437 conformations of lattice protein models by quantum annealing. *Scientific reports* **2012**, *2*, 571.
- 438 15. Sarkar, A. Quantum Algorithms: for pattern-matching in genomic sequences **2018**.
- 439 16. Biamonte, J.; Wittek, P.; Pancotti, N.; Rebentrost, P.; Wiebe, N.; Lloyd, S. Quantum machine learning.  
 440 *Nature* **2017**, *549*, 195.
- 441 17. Papalitsas, C.; Karakostas, P.; Andronikos, T.; Sioutas, S.; Giannakis, K. Combinatorial GVNS (General  
 442 Variable Neighborhood Search) Optimization for Dynamic Garbage Collection. *Algorithms* **2018**, *11*, 38.
- 443 18. Rebentrost, P.; Schuld, M.; Wossnig, L.; Petruccione, F.; Lloyd, S. Quantum gradient descent and Newton’s  
 444 method for constrained polynomial optimization. *New Journal of Physics* **2019**.
- 445 19. D-Wave, S. Getting Started with the D-Wave System. Technical report, D-Wave Systems, 2019.

- 446 20. Boothby, K.; Bunyk, P.; Raymond, J.; Roy, A. Next-generation topology of D-Wave quantum processors.  
447 Technical report, D-Wave Systems, 2019.
- 448 21. Dattani, N.; Szalay, S.; Chancellor, N. Pegasus: The second connectivity graph for large-scale quantum  
449 annealing hardware. *arXiv preprint arXiv:1901.07636* **2019**.
- 450 22. Dattani, N.; Chancellor, N. Embedding quadratization gadgets on Chimera and Pegasus graphs. *arXiv*  
451 *preprint arXiv:1901.07676* **2019**.
- 452 23. Boros, E.; Crama, Y.; Hammer, P.L. Upper-bounds for quadratic 0–1 maximization. *Operations Research*  
453 *Letters* **1990**, *9*, 73–79.
- 454 24. Lewis, M.; Glover, F. Quadratic unconstrained binary optimization problem preprocessing: Theory and  
455 empirical analysis. *Networks* **2017**, *70*, 79–97.
- 456 25. Kochenberger, G.; Hao, J.K.; Glover, F.; Lewis, M.; Lü, Z.; Wang, H.; Wang, Y. The unconstrained binary  
457 quadratic programming problem: a survey. *Journal of Combinatorial Optimization* **2014**, *28*, 58–81.
- 458 26. Lloyd, S.; Mohseni, M.; Rebentrost, P. Quantum algorithms for supervised and unsupervised machine  
459 learning. *arXiv preprint arXiv:1307.0411* **2013**.
- 460 27. Hauke, P.; Katzgraber, H.G.; Lechner, W.; Nishimori, H.; Oliver, W.D. Perspectives of quantum annealing:  
461 Methods and implementations. *arXiv preprint arXiv:1903.06559* **2019**.
- 462 28. Glover, F.; Kochenberger, G. A Tutorial on Formulating QUBO Models. *arXiv preprint arXiv:1811.11538*  
463 **2018**.
- 464 29. Boros, E.; Hammer, P.L.; Tavares, G. Local search heuristics for quadratic unconstrained binary optimization  
465 (QUBO). *Journal of Heuristics* **2007**, *13*, 99–132.
- 466 30. Ushijima-Mwesigwa, H.; Negre, C.F.; Mniszewski, S.M. Graph partitioning using quantum annealing  
467 on the D-Wave system. Proceedings of the Second International Workshop on Post Moores Era  
468 Supercomputing. ACM, 2017, pp. 22–29.
- 469 31. Newell, G.F.; Montroll, E.W. On the theory of the Ising model of ferromagnetism. *Reviews of Modern Physics*  
470 **1953**, *25*, 353.
- 471 32. Lucas, A. Ising formulations of many NP problems. *Frontiers in Physics* **2014**, *2*, 5.
- 472 33. Neukart, F.; Compostella, G.; Seidel, C.; Von Dollen, D.; Yarkoni, S.; Parney, B. Traffic flow optimization  
473 using a quantum annealer. *Frontiers in ICT* **2017**, *4*, 29.
- 474 34. Martoňák, R.; Santoro, G.E.; Tosatti, E. Quantum annealing of the traveling-salesman problem. *Physical*  
475 *Review E* **2004**, *70*, 057701.
- 476 35. Warren, R.H. Adapting the traveling salesman problem to an adiabatic quantum computer. *Quantum*  
477 *information processing* **2013**, *12*, 1781–1785.
- 478 36. Warren, R.H. Small traveling salesman problems. *Journal of Advances in Applied Mathematics* **2017**, *2*.
- 479 37. Feld, S.; Roch, C.; Gabor, T.; Seidel, C.; Neukart, F.; Galter, I.; Mauerer, W.; Linnhoff-Popien, C. A hybrid  
480 solution method for the capacitated vehicle routing problem using a quantum annealer. *arXiv preprint*  
481 *arXiv:1811.07403* **2018**.
- 482 38. Irie, H.; Wongpaisarnsin, G.; Terabe, M.; Miki, A.; Taguchi, S. Quantum annealing of vehicle routing  
483 problem with time, state and capacity. International Workshop on Quantum Technology and Optimization  
484 Problems. Springer, 2019, pp. 145–156.
- 485 39. Neven, H.; Denchev, V.S.; Rose, G.; Mcready, W.G. Training a large scale classifier with the quantum  
486 adiabatic algorithm. *arXiv preprint arXiv:0912.0779* **2009**.
- 487 40. Garnerone, S.; Zanardi, P.; Lidar, D.A. Adiabatic quantum algorithm for search engine ranking. *Physical*  
488 *review letters* **2012**, *108*, 230506.
- 489 41. Cruz-Santos, W.; Venegas-Andraca, S.; Lanzagorta, M. A QUBO Formulation of the Stereo Matching  
490 Problem for D-Wave Quantum Annealers. *Entropy* **2018**, *20*, 786.
- 491 42. Babbush, R.; Love, P.J.; Aspuru-Guzik, A. Adiabatic quantum simulation of quantum chemistry. *Scientific*  
492 *reports* **2014**, *4*, 6603.
- 493 43. Crispin, A.; Syriachas, A. Quantum annealing algorithm for vehicle scheduling. 2013 IEEE International  
494 Conference on Systems, Man, and Cybernetics. IEEE, 2013, pp. 3523–3528.
- 495 44. Cai, B.B.; Zhang, X.H. Hybrid Quantum Genetic Algorithm and Its Application in VRP [J]. *Computer*  
496 *Simulation* **2010**, *7*.
- 497 45. Binder, K.; Young, A.; Fischer, K.; Hertz, J. *Rev. Mod. Phys.*, 1986.
- 498 46. Young, A.P. *Spin glasses and random fields*; Vol. 12, World Scientific, 1998.



- 499 47. Nishimori, H. *Statistical physics of spin glasses and information processing: an introduction*; Number 111,  
500 Clarendon Press, 2001.
- 501 48. Venturelli, D.; Mandra, S.; Knysh, S.; O’Gorman, B.; Biswas, R.; Smelyanskiy, V. Quantum optimization of  
502 fully connected spin glasses. *Physical Review X* **2015**, *5*, 031040.
- 503 49. Titiloye, O.; Crispin, A. Quantum annealing of the graph coloring problem. *Discrete Optimization* **2011**,  
504 *8*, 376–384.
- 505 50. Venturelli, D.; Marchand, D.J.; Rojo, G. Quantum annealing implementation of job-shop scheduling. *arXiv*  
506 *preprint arXiv:1506.08479* **2015**.
- 507 51. Benedetti, M.; Realpe-Gómez, J.; Biswas, R.; Perdomo-Ortiz, A. Quantum-assisted learning of  
508 hardware-embedded probabilistic graphical models. *Physical Review X* **2017**, *7*, 041052.
- 509 52. Battaglia, D.A.; Santoro, G.E.; Tosatti, E. Optimization by quantum annealing: Lessons from hard  
510 satisfiability problems. *Physical Review E* **2005**, *71*, 066707.
- 511 53. Alom, M.Z.; Van Essen, B.; Moody, A.T.; Widemann, D.P.; Taha, T.M. Quadratic Unconstrained Binary  
512 Optimization (QUBO) on neuromorphic computing system. 2017 International Joint Conference on Neural  
513 Networks (IJCNN). IEEE, 2017, pp. 3922–3929.
- 514 54. Pagano, G.; Bapat, A.; Becker, P.; Collins, K.; De, A.; Hess, P.; Kaplan, H.; Kyprianidis, A.; Tan, W.; Baldwin,  
515 C.; others. Quantum Approximate Optimization with a Trapped-Ion Quantum Simulator. *arXiv preprint*  
516 *arXiv:1906.02700* **2019**.
- 517 55. Farhi, E.; Harrow, A.W. Quantum supremacy through the quantum approximate optimization algorithm.  
518 *arXiv preprint arXiv:1602.07674* **2016**.
- 519 56. Venegas-Andraca, S.E.; Cruz-Santos, W.; McGeoch, C.; Lanzagorta, M. A cross-disciplinary introduction to  
520 quantum annealing-based algorithms. *Contemporary Physics* **2018**, *59*, 174–197.
- 521 57. Farhi, E.; Goldstone, J.; Gutmann, S. A quantum approximate optimization algorithm. *arXiv preprint*  
522 *arXiv:1411.4028* **2014**.
- 523 58. Hadfield, S.; Wang, Z.; O’Gorman, B.; Rieffel, E.G.; Venturelli, D.; Biswas, R. From the quantum  
524 approximate optimization algorithm to a quantum alternating operator ansatz. *Algorithms* **2019**, *12*, 34.
- 525 59. Vyskocil, T.; Djidjev, H. Embedding Equality Constraints of Optimization Problems into a Quantum  
526 Annealer. *Algorithms* **2019**, *12*. doi:10.3390/a12040077.
- 527 60. Barán, B.; Villagra, M. A Quantum Adiabatic Algorithm for Multiobjective Combinatorial Optimization.  
528 *Axioms* **2019**, *8*, 32.
- 529 61. Oliveira, N.M.D.; Silva, R.M.D.A.; Oliveira, W.R.D. QUBO formulation for the contact map overlap  
530 problem. *International Journal of Quantum Information* **2018**, *16*, 1840007.
- 531 62. Rosenberg, G.; Vazifeh, M.; Woods, B.; Haber, E. Building an iterative heuristic solver for a quantum  
532 annealer. *Computational Optimization and Applications* **2016**, *65*, 845–869.
- 533 63. Langevin, A.; Desrochers, M.; Desrosiers, J.; Gélinas, S.; Soumis, F. A two-commodity flow formulation for  
534 the traveling salesman and the makespan problems with time windows. *Networks* **1993**, *23*, 631–640.
- 535 64. Dumas, Y.; Desrosiers, J.; Gelin, E.; Solomon, M.M. An optimal algorithm for the traveling salesman  
536 problem with time windows. *Operations research* **1995**, *43*, 367–371.
- 537 65. Gendreau, M.; Hertz, A.; Laporte, G.; Stan, M. A generalized insertion heuristic for the traveling salesman  
538 problem with time windows. *Operations Research* **1998**, *46*, 330–335.
- 539 66. Da Silva, R.F.; Urrutia, S. A General VNS heuristic for the traveling salesman problem with time windows.  
540 *Discrete Optimization* **2010**, *7*, 203–211.
- 541 67. Sotiropoulos, D.; Stavropoulos, E.; Vrahatis, M. A new hybrid genetic algorithm for global optimization.  
542 *Nonlinear Analysis: Theory, Methods & Applications* **1997**, *30*, 4529–4538.
- 543 68. Pardalos, P.M.; Rodgers, G.P. Computational aspects of a branch and bound algorithm for quadratic  
544 zero-one programming. *Computing* **1990**, *45*, 131–144.
- 545 69. Lahoz-Beltra, R. Quantum genetic algorithms for computer scientists. *Computers* **2016**, *5*, 24.
- 546 70. Papalitsas, Ch.; Giannakis, K.; Andronikos, Th.; Theotokis, D.; Sifaleras, A. Initialization methods for  
547 the TSP with Time Windows using Variable Neighborhood Search. IEEE Proc. of the 6th International  
548 Conference on Information, Intelligence, Systems and Applications (IISA 2015), 6-8 July, Corfu, Greece,  
549 2015.
- 550 71. Papalitsas, C.; Karakostas, P.; Kastampolidou, K. A Quantum Inspired GVNS: Some Preliminary Results.  
551 GeNeDis 2016; Vlamos, P., Ed.; Springer International Publishing: Cham, 2017; pp. 281–289.

- 552 72. Papalitsas, C.; Andronikos, T. Unconventional GVNS for Solving the Garbage Collection Problem with  
553 Time Windows. *Technologies* **2019**, *7*. doi:10.3390/technologies7030061.
- 554 73. Ohlmann, J.W.; Thomas, B.W. A compressed-annealing heuristic for the traveling salesman problem with  
555 time windows. *INFORMS Journal on Computing* **2007**, *19*, 80–90.
- 556 74. Vyskočil, T.; Pakin, S.; Djidjev, H.N. Embedding Inequality Constraints for Quantum Annealing  
557 Optimization. *Quantum Technology and Optimization Problems*; Feld, S.; Linnhoff-Popien, C., Eds.;  
558 Springer International Publishing: Cham, 2019; pp. 11–22.